SUPPLEMENTAL DATA

Relative stereociliary motion in a hair bundle opposes amplification at distortion frequencies

Andrei S. Kozlov,[1] Thomas Risler,[1,2,3,4] Armin J. Hinterwirth,[1] and A. J. Hudspeth[1]

[1]Howard Hughes Medical Institute and Laboratory of Sensory Neuroscience, The Rockefeller University, New York, New York; [2]Institut Curie, Centre de Recherche, F-75005, Paris, France; [3]UPMC Université Paris 06, UMR 168, F-75005, Paris, France; [4]CNRS, UMR 168, F-75005, Paris, France

The experiments presented in the main text were performed on hair cells from the bullfrog's sacculus, an organ responsive to frequencies around 100 Hz (Lewis, 1988). We wished to test the generality of our previous conclusion that hair cells display high coherence (Kozlov et al., 2007) in auditory hair bundles tuned to higher frequencies. For this purpose we recorded from hair bundles of the basilar papilla in the tokay gecko (*Gekko gecko*), a lizard with a well developed sense of hearing that extends to about 7 kHz (Manley, 1972).

Cochleae dissected from geckos (Chiappe et al., 2007) were maintained in oxygenated saline solution comprising 170 mM NaCl, 2 mM KCl, 1 mM $CaCl_2$, 10 mM **D**-glucose, and 5 mM HEPES at pH 7.3. After a 30-60 min digestion of basilar papillae at room temperature in 1 mg/ml collagenase (type XI, Sigma Chemical Co.), hair cells were mechanically isolated with an eyelash and allowed to settle onto the bottom of an experimental chamber coated with either concanavalin A (Sigma) or Cell-Tak (BD Biosciences) to promote cellular adhesion.

A typical pair of time series obtained from the opposite edges of a gecko's hair bundle demonstrated fluctuations with a root-mean square (RMS) magnitude of 3.5 ± 0.5 nm

(mean ± standard deviation; Fig. S1A). The associated spectra showed a high coherence across the hair bundle with a phase difference near zero at all frequencies (Fig. S1B). A complete measurement, which comprised twenty such records, yielded similar coherence and phase spectra (Fig. S1C). These results did not differ significantly from those obtained with the two laser beams superimposed at the same position on the hair bundle (Fig. S1D). The average coherence and phase spectra obtained from five hair bundles confirm the consistency of the results (Fig. S2).

Measurements of coherency from isolated hair cells may be corrupted by whole-cell drift. We therefore performed on each isolated cell a control measurement in which one laser beam was positioned on the hair bundle and the other on the apical portion of the cell body. If the two signals displayed cross-correlations above the background noise level, the cell was rejected from further analysis. For the five cells included in the analysis, the average coherence between measurements from cell bodies and the associated hair bundles was 0.2 ± 0.1 and the average phase was 0.0 ± 1.7 rad between 100 Hz and 5 kHz. This result is consistent with the expectation for two independent signals. In contrast, when the two laser beams were positioned on the opposite sides of these hair bundles, the coherence was 0.88 ± 0.07 and the phase was 0.0 ± 0.1 rad (Fig. S2). These values indicate that auditory hair bundles from the tokay gecko move with a high coherence.

Experimental studies of hair-bundle kinematics with high resolution in isolated cells suffer from at least three methodological drawbacks: cell isolation may cause excessive mechanical and metabolic damage; the proximity of a hair bundle to the recording chamber's glass surface may affect the hydrodynamic forces experienced by the stereocilia; and isolated cells may drift with the local hydrodynamic flow. Although drifting could be strongly reduced by covering the recording chamber with adhesive substances such as concanavalin A and Cell-Tak, most cells nevertheless displayed whole-cell motions of several tens of nanometers. Because these movements were large compared with those typical of relative stereociliary motions, they dominated the measurements. When their global motion was negligible, we could use some

isolated cells for recordings of hair-bundle motion. However, stimulating isolated cells with a patch pipette attached to their hair bundles displaced the cell bodies too much to allow reliable measurements of the relative stereociliary motion. Because the basilar papilla of the tokay gecko is thin, with only a dozen hair cells abreast, we could not fold it to provide optical access to laterally protruding hair bundles without damaging the cells. For these reasons, we report in the main text the results from our experiments with the bullfrog's sacculus, which has the advantage of being mechanically stable and metabolically robust: we occasionally observed hair bundles oscillating spontaneously for as long as 20 hours *in vitro*.

Choice of the multitaper spectral-analysis technique

The structure of the data was investigated through linear frequency-domain representations using the multitaper spectral-estimation method (Thomson, 1982; Percival and Walden, 1993). This choice is motivated by the observation that standard spectral-estimation methods based on single data windows suffer from two fundamental problems, namely bias and lack of consistency of the so-obtained estimates. The first problem refers to the fact that the estimate of the spectral quantity at a given frequency mixes information from different frequency components of the original signal. The second problem refers to the fact that the variance of the estimate does not decline with an increasing sample size, for the outcome contains as many quantities as there are data values. Data tapering by a single window, which is often used in an attempt to solve the first problem, suffers from variance-efficiency reduction, unequal weighting of the data, and arbitrariness in taper selection (Brillinger, 1981; Thomson, 1982). In our case, the bias reduction offered by the use of a single window was also inadequate because our records contained a relatively important part of low-frequency signal that was unrelated to the desired observations and that could have contaminated the frequency components of interest. To solve the second problem, a convolution product in the frequency domain could be used to smooth the desired estimates, but this operation relies on the assumption that the output spectral quantities are

smooth. In our case the spectral power was concentrated at specific frequencies and this condition was unsatisfied.

Details of the multitaper spectral analysis

Any stationary stochastic process $X(t)$ sampled at a rate τ can be characterized by its Cramer spectral representation

$$X(t) = \int_{-1/(2\tau)}^{1/(2\tau)} \mathrm{d}X(f) e^{2\pi i f t} \tag{1}$$

for any time t at which it is sampled. Here $\mathrm{d}X(f)$ is an orthogonal-increment process: for zero-mean processes $E\{\mathrm{d}X(f)\} = 0$; for distinct frequencies f_1 and f_2, $\mathrm{d}X(f_1)$ and the complex conjugate of $\mathrm{d}X(f_2)$ are statistically uncorrelated. The second moment of this function defines the power spectrum $S(f)$ of the process,

$$S(f)\mathrm{d}f = E\left\{\left|\mathrm{d}X(f)\right|^2\right\}. \tag{2}$$

In actual experiments, however, we can observe only a specific realization $x(t)$ of $X(t)$ and can do so only over the finite time window $T = N\tau$. The observed time series $\tilde{x}(t)$ has a Fourier transform $\tilde{x}(f)$ that is related to the Fourier transform $x(f)$ of the infinite time series $x(t)$ by

$$\tilde{x}(f) = \sum_{j=1}^{N} x(t_j) e^{-2\pi i f t_j} = \int_{-1/(2\tau)}^{1/(2\tau)} K(f - f', N) x(f') \mathrm{d}f', \tag{3}$$

in which $t_j = j\tau$ and

$$K(f) = e^{-\pi i f (N+1)} \left[\frac{\sin(N\pi f)}{\sin(\pi f)} \right]. \tag{4}$$

For a stationary stochastic process the spectrum can be estimated as $\left|\tilde{x}(f)\right|^2$, the squared Fourier transform of the data series. However, $\tilde{x}(f)$ is not equal to $x(f)$ but is related to it by a convolution product that mixes information originating in different frequency channels (Equation 3); this corresponds to the first problem of bias mentioned above. Moreover, $\left|\tilde{x}(f)\right|^2$ squares the observations without averaging them, estimating N quantities from N data values.

The resultant over-fitting problem corresponds to the second problem mentioned above, namely lack of consistency.

The multitaper spectral-estimation method provides an elegant solution to both problems (Thomson, 1982; Percival and Walden, 1993). In this approach, the data are multiplied not by a single window but rather by a set of K optimally chosen data tapers $w_k(t)$. The power spectrum is then estimated as

$$S_{\mathrm{MT}}(f) = \frac{1}{K}\sum_{k=1}^{K}\left|\tilde{x}_k(f)\right|^2, \tag{5}$$

in which

$$\tilde{x}_k(f) = \sum_{j=1}^{N} w_k(t_j)x(t_j)e^{-2\pi i f t_j}. \tag{6}$$

The optimal choice of the taper functions requires that they be mutually orthogonal, providing K independent spectral estimates, and that they possess maximal spectral concentration, yielding the greatest relative power over the frequency bandwidth $2W$ (Mitra and Pesaran, 1999). The spectral concentration value is quantified by

$$\lambda_k(N,W) = \frac{\int_{-W}^{W}\left|U_k(f)\right|^2 \mathrm{d}f}{\int_{-1/(2\tau)}^{1/(2\tau)}\left|U_k(f)\right|^2 \mathrm{d}f}, \tag{7}$$

in which $U_k(f)$ is the Fourier transform of the sequence $w_k(t)$ and τ is the sampling rate. It can be shown that $\lambda_k(N,W)$ is the k^{th} eigenvalue of the eigenvector relation

$$\sum_{j'=1}^{N}\frac{\sin\left[2\pi W(t_j - t_{j'})\right]}{\pi(t_j - t_{j'})}w(t_{j'}) = \lambda w(t_j); \tag{8}$$

$w_k(t)$ corresponds to the associated eigenvector under appropriate normalization.

These optimal taper functions have the remarkable property that $2NW\tau$ of their eigenvalues are approximately equal to one, whereas the remainder decay sharply to zero (Slepian and Pollak, 1961; Slepian, 1978). As a result, the spectrum is convolved with a window that is as close as possible to a rectangular shape, yielding a power-spectral estimate that results at each frequency f_0 from an equally weighted average of contributions across the frequency

band $\left[f_0 - W, f_0 + W\right]$. At the same time, leakage to and from frequencies outside this frequency band is as small as possible.

We chose as the final spectral estimate an equally weighted average of the different tapered spectra. Although more sophisticated techniques of averaging can be implemented with both frequency- and data-dependent weighting (Thomson, 1982; Percival and Walden, 1993; Mitra and Pesaran, 1999), these approaches significantly affect the results only when tapers with poor spectral concentration are used. Because we could average over several independent records for each measurement, we did not need to include a large number of tapers to obtain consistent estimates. We could therefore restrict ourselves to tapers with high concentration properties, rendering adaptive-weighting techniques superfluous.

Jackknife error estimation

The multitaper method also permits calculation of the variance of an estimated spectrum by means of jackknifing (Thomson and Chave, 1991). Although this method is applicable to relatively complicated data, it is largely free of distributional assumptions and hence highly reliable. Moreover, the jackknife variance always exceeds the true variance, so the estimates are conservative (Efron and Stein, 1981).

The jackknife approach was implemented as follows. Let $\left\{x_i\right\}$, $i = 1,...,P$ be a sample of P independent observations drawn from some distribution characterized by a parameter θ to be estimated, and let $\hat{\theta}$ be an estimate of θ. In addition to the usual estimate $\hat{\theta}_{\text{all}}$ based on all P observations, we formed P estimates $\left\{\hat{\theta}_{\setminus i}\right\}$, each based on the $(P-1)$ observations remaining after deletion of the i^{th} one. In the nonparametric estimation of the variance of an arbitrary statistics,

$$\text{var}\left(\hat{\theta}\right) = \frac{P-1}{P}\sum_{i=1}^{P}\left(\hat{\theta}_{\setminus i} - \theta_{\cap}\right)^2, \tag{9}$$

in which

$$\theta_{\cap} = \frac{1}{P}\sum_{i=1}^{P}\hat{\theta}_{\setminus i}. \tag{10}$$

These estimates require the use of transformations prior to jackknifing when the statistics is bounded or its distribution is strongly non-Gaussian, for example strongly asymmetrical about the mean value. We used the logarithmic transformation for jackknifing power spectra and the inverse hyperbolic transformation for jackknifing coherences (Thomson and Chave, 1991).

In power-spectral estimation, a logarithmic transformation stabilizes the distribution into a more symmetric one. Taking $\hat{\theta} = \ln\hat{S}$ as our estimator, we formed the delete-one values $\ln\hat{S}_{\setminus i}$ as

$$\ln\hat{S}_{\setminus i} = \ln\left(\frac{1}{P-1}\sum_{\substack{k=1\\k\neq i}}^{P}\hat{S}_k\right), \tag{11}$$

with their average

$$\ln S_{\cap} = \frac{1}{P}\sum_{i=1}^{P}\ln\hat{S}_{\setminus i} \tag{12}$$

defining a power-spectral estimate $S_{\cap}$. It follows that the jackknife estimate of the variance of the logarithmic power spectrum was

$$\hat{\sigma}^2 = \mathrm{var}\left\{\ln\hat{S}\right\} = \frac{P-1}{P}\sum_{i=1}^{P}\left(\ln\hat{S}_{\setminus i} - \ln S_{\cap}\right)^2. \tag{13}$$

Because of the logarithmic transformation, $\left(\ln\hat{S}_{\setminus i} - \ln S_{\cap}\right)/\hat{\sigma}$ was distributed nearly as t_{P-1}, a t-distribution with $P-1$ degrees of freedom. The approximate $(1-\alpha)$ confidence interval for the power spectrum was given by

$$\hat{S}e^{-t_{P-1}(1-\alpha/2)\hat{\sigma}} < S \leq \hat{S}e^{t_{P-1}(1-\alpha/2)\hat{\sigma}}. \tag{14}$$

Coherence and phase estimation

To jackknife coherence and phase spectral estimates, we assumed the availability of P complex transform pairs, $x_k(f)$ and $y_k(f)$. We defined the delete-one estimates of the coherency as

$$\hat{c}_{\setminus j} = \frac{\sum_{\substack{k=1 \\ k \neq j}}^{P} x_k(f) y_k^*(f)}{\left[\sum_{\substack{k=1 \\ k \neq j}}^{P} |x_k(f)|^2 \sum_{\substack{k=1 \\ k \neq j}}^{P} |y_k(f)|^2 \right]^{1/2}} \tag{15}$$

for $j = 1,2,...,P$, plus the standard estimate with nothing omitted (Thomson and Chave, 1991). From these, we transformed to the almost normal variates

$$Q_{\setminus j} = \sqrt{2P-2} \tanh^{-1}\left(\left| \hat{c}_{\setminus j} \right| \right) \tag{16}$$

and obtained estimates and tolerances of the coherence spectrum.

Delete-one phase factors were constructed as

$$e_{\setminus j} = \frac{\hat{c}_{\setminus j}}{\left| \hat{c}_{\setminus j} \right|}, \tag{17}$$

with an average value

$$e_{\cap} = \frac{1}{P} \sum_{j=1}^{P} e_{\setminus j} . \tag{18}$$

This approach provided an estimate of the phase variance as

$$V\left\{ \hat{\phi} \right\} = 2(P-1) \cdot \left(1 - \left| \phi_{\cap} \right| \right), \tag{19}$$

in which $\phi_{\cap} = \arg\left\{ e_{\setminus j} \right\}$, an application of the jackknife method to standard phase statistics (Fisher, 1993). In particular, the estimate took periodicity into account and was equivalent to

$$\frac{P-1}{P} \sum_{j=1}^{P} \left(\phi_{\setminus j} - \phi_{\cap} \right)^2, \tag{20}$$

in which $\phi_{\setminus j} = \arg\left\{ e_{\setminus j} \right\}$ for small phase dispersion.

REFERENCES

Brillinger, D. R. (1981). The key role of tapering in spectrum estimation. IEEE Trans. Acoust., Speech, Signal Processing ASSP-29, 1075-1076.

Chiappe, M. E., Kolzov, A. S. & Hudspeth A. J. (2007). The structural and functional

differentiation of hair cells in a lizard's basilar papilla suggests an operational principle of amniote cochleas. J. Neurosci. 27, 11978–11985.

Efron, B. & Stein, C. (1981). The jackknife estimate of variance. Ann. Statist. 9, 586–596.

Kozlov, A. S., Risler, T. & Hudspeth, A. J. (2007). Coherent motion of stereocilia assures the concerted gating of hair-cell transduction channels. Nature Neurosci. 10, 87–92.

Lewis, E. R. (1988). Tuning in the bullfrog ear. Bioph. J. 53, 441–447.

Manley, G. (1972). Frequency response of the ear of the Tokay gecko. J. Exp. Zool. 181, 159–168.

Mitra, P. P. & Pesaran, B. (1999). Analysis of dynamic brain imaging data. Biophys. J. 76, 691–708.

Percival, D. B. & Walden, A. T. (1993). Spectral Analysis for Physical Applications: Multitaper and Conventional Univariate Techniques. (Cambridge University Press. Cambridge, UK).

Slepian, D. & Pollack, H. O. (1961). Prolate spheroidal wave functions, Fourier analysis, and uncertainty—I. Bell Syst. Techn. J. 40, 43–63.

Slepian, D. (1978). Prolate spheroidal wave functions, Fourier analysis, and uncertainty – V: The discrete case. Bell Syst. Techn. J. 57, 1371–1430.

Thomson, D. J. (1982). Spectrum estimation and harmonic analysis. Proc. IEEE. 70, 1055–1096.

Thomson, D. J. & Chave, A. D. (1991). Jackknifed error estimates for spectra, coherences, and transfer functions. In Advances in Spectrum Analysis and Array Processing 58–113 (Prentice Hall, Englewood Cliffs, NJ).

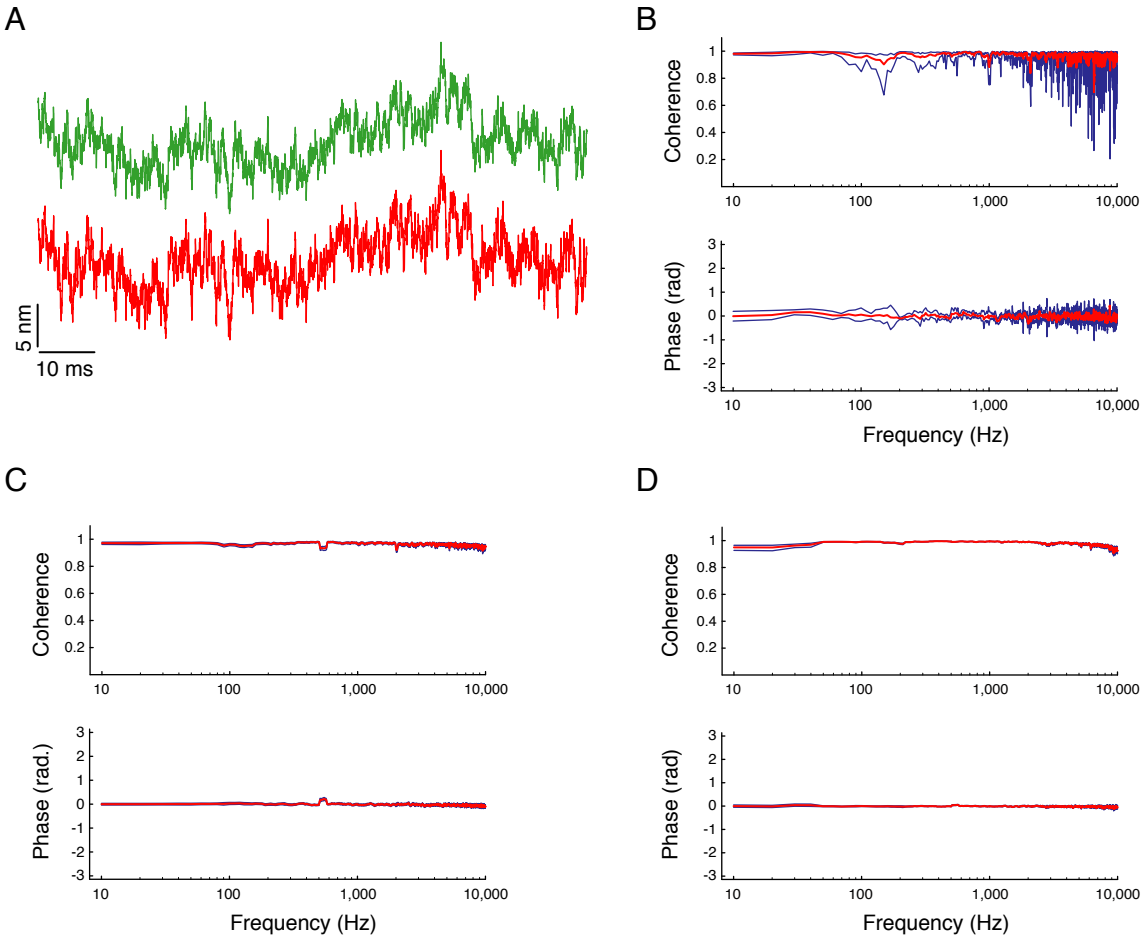
A
5 nm
10 ms
B
Coherence
Phase (rad)
Frequency (Hz)
C
Coherence
Phase (rad.)
Frequency (Hz)
D
Coherence
Phase (rad)
Frequency (Hz)

Figure S1: Time series and coherency spectra from an auditory hair bundle. (A) Simultaneous recordings with two interferometric beams show highly similar patterns of motion at the opposite edges of a gecko's hair bundle. (B) The coherence and phase spectra for the records in panel (A) are shown in red, together with their associated 95 % confidence intervals in blue. (C) Averaging the coherence and phase spectra from 20 records for the opposite edges of the same hair bundle greatly reduces the experimental uncertainty. The confidence intervals were obtained by jackknifing the entire set of records. (D) The average spectra from 20 records with the two beams positioned at an identical position in the same hair bundle closely resemble those in panel (C).

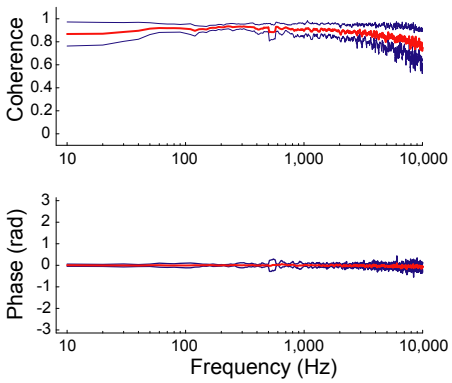
Coherence
1
0.8
0.6
0.4
0.2
0
10
100
1,000
10,000
Phase (rad)
3
2
1
0
-1
-2
-3
10
100
1,000
10,000
Frequency (Hz)

Figure S2: Coherence and phase spectra from auditory hair bundles. The figure displays the average values (red) and the associated standard deviations (blue) of the coherence and phase spectra for recordings from the opposite edges of five hair bundles from the gecko's basilar papilla.